International Journal of Current Bio-Medical Engineering (IJCBE)
Volume 2, Issue 1, January – February (2024)

RESEARCH ARTICLE

MLSIA-LC: DEEP LEARNING-BASED MULTI-LEVEL SELF AND INTER-ATTENTION NETWORKS FOR LUNG CANCER CLASSIFICATION

P. William [1, *], Abdulatif Alabdultif [2]

[1] School of Engineering and Technology, Sanjivani University, Kopargaon, Maharashtra, India.
[2] Department of Computer Science, College of Computer, Qassim University, Buraydah 52571, Saudi Arabia.
[*]*Corresponding e-mail: william160891@gmail.com*

Abstract – Lung cancer is among the world's leading causes of death and its accurate and early diagnosis is critical for effective treatment planning. However, lung cancer often presents subtle early symptoms, making early detection challenging, and its diagnosis relies heavily on imaging techniques that can sometimes miss small or irregular nodules. To overcome these challenges a novel MLSIA-LC has been proposed deep learning-based Multi-Level Self and Inter-Attention (MLSIA) Network for the classification of lung cancer subtypes using CT and PET scan images. Then the segmentation of lung nodules using the Attention U-Net model. Advanced texture patterns, namely Directional Hexagonal Inter Mixed Pattern (DHIMP) and Directional Hexagonal Inter-Intra Mixed Pattern (DHIIMP), are extracted from segmented regions to capture unique spatial features from both CT and PET images. These patterns are fed into a parallel network architecture comprising three pathways, each with two levels of Multi-Level Self-Attention (MLSA) networks and Inter-Attention layers, followed by dropout mechanisms to enhance feature. The experimental results of MLSIA network achieves higher classification performance compared to existing methods, particularly with the DHIIMP texture pattern. The proposed model achieved an accuracy of 92.1% and an F1 score of 90%, outperform effectively leveraging inter- and intra-pattern information.

Keywords *– Lung cancer, Attention U-Net, Multi-Level Self-Attention, Directional Hexagonal Inter Mixed Pattern, Directional Hexagonal Inter-Intra Mixed Pattern.*

1. INTRODUCTION

Cancer is a deadly ailment considered as an abnormal growth of anomalous cells that can infiltrate and destroy normal tissue. [1] The variation that occurs in the DNA leads to cancer and these disparities are also called genetic variations. Cancer cells generally behave differently from normal cells and can spread out to other parts of the body. [2] This spreading process of cancer cells to metastases to other regions of the body. [3] Cancer arises from the conversion of normal cells into malignant cells in a multi-stage procedure that gradually progresses from a pre-cancerous cell to a malignant cell. [4] A growing number of non-communicable diseases are a major health concern due to different factors that includes lifestyle changes, urbanization, and globalization. [5] Estimating a load of cancer in terms of incidence and mortality at present and future is useful for planning cancer control strategies, risk estimation and measuring the population burden of cancer. [6] With the control of infectious and communicable diseases and increased life expectancy, more of the populations in India are at risk of developing cancer.

In deep learning models, CAD systems are developed with automatically extracted features to accurately classify the cancerous lungs [7]. LIDC is a large repository of lung cancer images that provides 1018 studies of computed tomography images which helps the deep learning researchers to effectively classify the abnormal lung nodules from the normal nodules [8]. But CT scan images include only the anatomical properties. In recent studies, the use of PET and CT scans for cancer detection has received higher attention. Lung cancer types accurately classified using non-invasive diagnostic imaging techniques such as PET and CT scans.

PET and CT scan images are given as input to the Attention U-Net for performing segmentation of lung nodules [9]. Using Directional hexagonal Inter mixed patterns (DHIMP) and Directional hexagonal Inter-Intra mixed patterns (DHIIMP) algorithms new texture patterns are generated from the segmented lung nodules. [10] In the proposed multi-level self and inter-attention (MLSIA) network model, features extracted from the PET and CT images are merged using parallel network architecture. [11] This model consists of three parallel networks with two multilevel networks each, as well as a self-attention network, an inter-attention network, and a dropout network. As a result of the dropout layer, the feature maps are mapped to lung

cancer categories by a more intrinsic adaptive average pooling technique. [12] It also avoids overfitting problems. [13] As lung cancer is so common, it can be difficult to detect false positives in imaging techniques like CT scans, leading to unnecessary procedures. Additionally, early-stage lung cancer often presents subtle symptoms, making early detection difficult. To overcome this problem, a novel MLSIA-LC model has been proposed for Lung cancer classification. The major research contributions are mentioned below;

- The research aims to create a novel deep learning-based MLSIA-LC used for classification of Lung cancer.
- Initially, the LC-input images CT and PET are fed in to Attention U-Net to segment lung nodules.
- Then the proposed method utilizes, hexagonal pattern generator is used for extracting feature from the Noise free images.
- Finally, MLSIA is used to classify types of Lung cancer namely Adenocarcinoma, Squamous Cell Carcinoma, Small Cell carcinoma, and Large Cell Carcinoma
- The proposed MLSIA-LC effectiveness was assessed using parameters like recall, specificity, accuracy, precision, and F1 score.

The remainder of this work has been scheduled as follows. A summary of the literature is provided in Section 2, followed by a full explanation of the proposed MLSIA-LC methodology for LC detection in Section 3, Section 4 contains the results and discussion, and Section 5 concludes with some future work.

2. LITERATURE SURVEY

In this section, the state-of-the-art in the domains that are pertinent to the work that is being presented, including data, deep learning, machine learning methods, and related studies. Related studies are listed in the following paragraphs, with an emphasis on those that make use of Lung cancer detection.

In 2017 Wulandari et al., [14] exploited several pre-processing methods for lung CT images to automatically detect lung cancer. The image was then subjected to morphological processing through erosion and dilation, giving it a smoother texture. The segmentation performance for calculating errors showed an average value of 12.75% for cavities and 31.74% for cancers.

In 2017 Nishio et al., [15] introduced the conventional auto-encoder (CAE) model in lung ultra-low-dose CT(ULDCT) images. The optimal denoising model was obtained by diminishing the cost function between the input images and the reconstructed images. These patches were then placed, and the overlapping sections were averaged to create the final image. The visual evaluation's findings demonstrate that the CAE method was superior at reducing noise artifacts.

In 2018 Perumal et al.,[16] applied contrast enhancement and noise removal techniques in MRI scans to increase the image quality. Image conversion was first performed into the grayscale format and then the dimensions of the images were enlarged or lessen. The experimental findings show that the Median filter outperforms other filter types like Wiener filter and Gaussian filter in terms of pixel intensity.

In 2020 Shakeel et al., [17] employed a weighted mean histogram equalization (WMHE) for enhancing the intensity of lung images during lung cancer prediction. Each pixel is compared to the upper limit value before the image quality is improved, and any noise is replaced with the middle value. Finally, an improved profuse clustering technique and a trained network was used to segment and categorized the processed image.

In 2021 Tasci et al., [18] devised a model for tuberculosis (TB) prognosis on basis of voting and preprocessing variation-based ensemble CNNs. In these techniques, weighted voting was used based on Bayesian optimization and the probability average. According to the computational findings, the proposed strategy applied to the Montgomery and Shenzhen datasets achieves accuracy rates of 97.5 percent and 97.6 percent respectively.

In 2021Sori et al., [19] designed a denoising first two-path CNN to reduce the noise in lung CT images. The retraining strategy was proposed to overcome the challenges brought about by the imbalance in image labels. This model diminishes the artifacts from the images by adjusting the inconsistent relationships between nodule shape and size, balancing the influence of receptive field size.

In 2015 Miah et al., [20] suggested a two-stage technique for detecting lung cancer in its initial stages. The segmenting the right and left lungs using a series of processes, including edge detection, dilated conversion, and image filling. This network was trained with the extracted features and it was assessed on both malicious and normal images. 150 lung CT scans were used in this testing, and the overall accuracy performance was 96.67%.

In literature review, a several methods for identifying lung cancer were centered on single input images and high computational costs, limited scalability. Additionally, early-stage lung cancer often presents subtle symptoms, making early detection difficult. To overcome these challenges, a novel MLSIA-LC introduce for accurate classification of Lung cancer.

3. PROPOSED METHODOLOGY

In this research, a novel MLSIA-LC model is proposed for classifying the Lung cancer classification from the dataset. Figure.1 shows the general process of the proposed MLSIA-LC methodology.

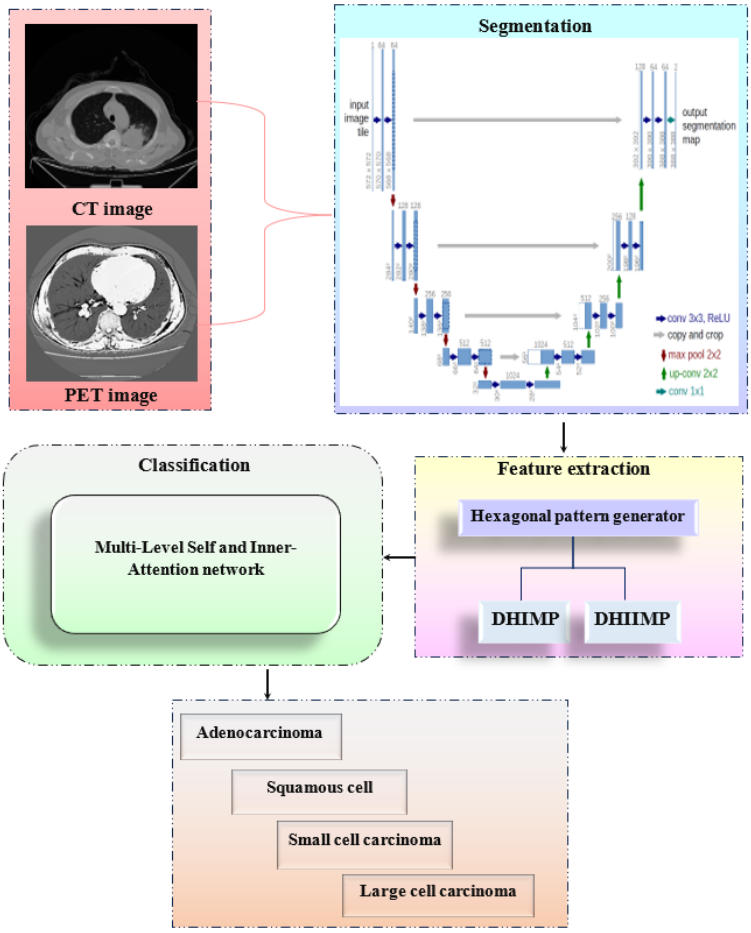

Figure 1. The Proposed MLSIA-LC method

3.1 Dataset Description

The dataset includes 363 cases, each categorized into four groups based on histological diagnosis: Radiologists marked 29,121 slices as cancerous, with 7894 slices from group A, 3116 slices from group B, 1005 slices from group E, and 4310 slices from group G. To increase the E group, a data augmentation procedure was applied, selecting 16,325 slices for further processing, with 80% for training and 20% for testing.

3.2 Segmentation

Processing the raw scan images may not produce accurate classifications as they have some noise disturbances and also it may not identify the nodule masses present near the border of the lung tissue.

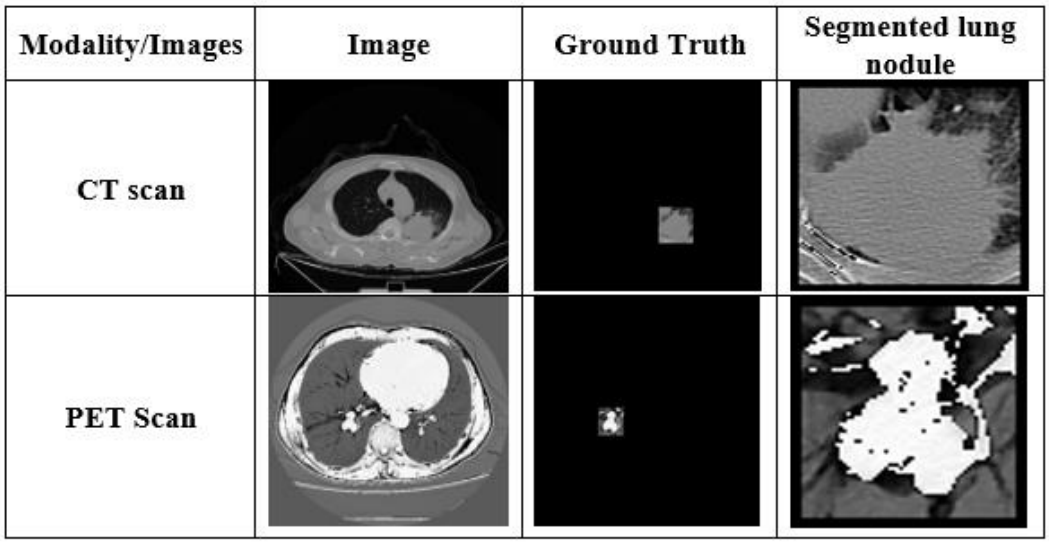

Figure 2. A sample of CT and PET scan images with the segmented lung nodule

In this Attention U-Net architecture is used to implement the segmentation of PET and CT scan images. Figure 2shows a sample of CT and PET scan images with the ground truth and segmented lung nodule.

3.3 Hexagonal pattern Generation

Hexagonal pattern Generation important to collect more detailed information about a definite region by considering the hexagonal texture features in addition to the color, shape, and size. The flow of hexagonal feature generation is shown in Figure. 3

The pixel values are selected in the clockwise direction. If the value of neighbour pixel value is higher than the value of centre pixel, then replace the grey-scale value with one or else zero. The new pattern generation algorithms were covered in more detail in the section that follows.

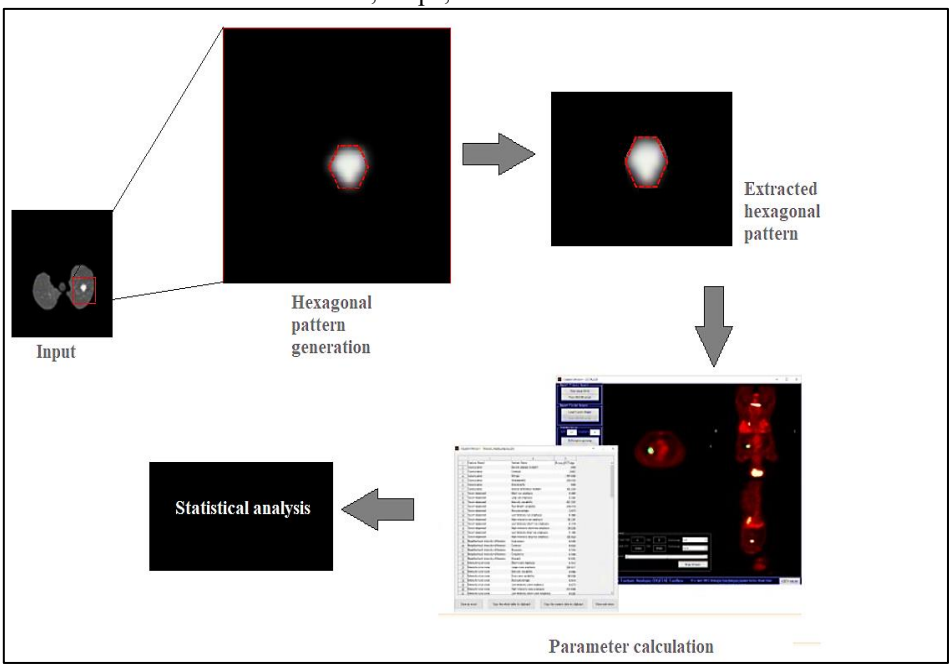

Figure 3. Hexagonal textural analysis

3.3.1 Directional Hexagonal Inter Mixed Pattern

In the DHIMP pattern, consider both CT and PET scan images. Every case in the dataset has a CT volume and a PET volume, from which we segment the pulmonary nodules. The center pixel value is considered from a particular cell in the CT image, remaining adjacent left, right, upper, and lower values are chosen from the PET images.

x-4,y-4	x-4,y-3	x-4,y-2	x-4,y-1	P(x-4,y)	x-4,y+1	x-4,y+2	x-4,y+3	x-4,y+4
x-3,y-4	x-3,y-3	x-3,y-2	P(x-3,y-1)	x-3,y	P(x-3,y+1)	x-3,y+2	x-3,y+3	x-3,y+4
x-2,y-4	x-2,y-3	x-2,y-2	P(x-2,y-1)	C(x-2,y)	P(x-2,y+1)	x-2,y+2	x-2,y+3	x-2,y+4
x-1,y-4	P(x-1,y-3)	P(x-1,y-2)	C(x-1,y-1)	P(x-1,y)	C(x-1,y+1)	P(x-1,y+2)	P(x-1,y+3)	x-1,y+4
P(x,y-4)	x,y-3	x,y-2	P(x,y-1)	C(x,y)	P(x,y+1)	x,y+2	x,y+3	P(x,y+4)
x+1,y-4	P(x+1,y-3)	P(x+1,y-2)	C(x+1,y-1)	P(x+1,y)	C(x+1,y+1)	P(x+1,y+2)	P(x+1,y+3)	x+1,y+4
x+2,y-4	x+2,y-3	x+2,y-2	P(x+2,y-1)	C(x+2,y)	P(x+2,y+1)	x+2,y+2	x+2,y+3	x+2,y+4
x+3,y-4	x+3,y-3	x+3,y-2	P(x+3,y-1)	x+3,y	P(x+3,y+1)	x+3,y+2	x+3,y+3	x+3,y+4
x+4,y-4	x+4,y-3	x+4,y-2	x+4,y-1	P(x+4,y)	x+4,y+1	x+4,y+2	x+4,y+3	x+4,y+4

Figure 4. Pixel selection in Directional Hexagonal Inter Mixed Pattern

The clear representation of selecting all the five sets of hexagonal bits is shown in Figure.3 As shown in Figure. 4, C (x, y) is the center pixels selected from the CT scan images and P (x, y) denote the pixels selected from the PET scan images. The decimal to binary bit conversion is generally expressed as Equation (1)

$$M_{MI}(G_i, G_c) = \begin{cases} 0 \; G_i < G_c \\ 1 \; G_i < G_c \end{cases} \quad (1)$$

Here the converted image is represented as M_{MI}, G_c is the center pixel value and G_i is the neighbor pixel values. Perform XOR operation on the converted bit values to produce partial bits as shown in Equations (2) - (5). The partial bits are combination of two opposite directions. '⊕' denotes XOR operation.

$$[uplo_0 \dots uplo_2] = [up_0 \dots up_2]$$

$$[uplo_0 \dots uplo_5] = [up_3 \dots up_5] \oplus [lo_3 \dots lo_5] \quad (2)$$

The list '$uplo$' is the combination of upper- and lower-bit values. The first three bits of the list '$uplo$' are the first three values of the list 'up'. Follow the same to generate the list 'rile' for the right and left values as shown in the Equation (3).

$$[rile_0 \dots rile_2] = [ri_0 \dots ri_2]$$

$$[rile_3 \dots rile_5] = [ri_3 \dots ri_5] \oplus [le_3 \dots le_5] \quad (3)$$

$$[loup_0 \dots loup_2] = [lo_0 \dots lo_2] \oplus [up_0 \dots up_2] \quad (4)$$

$$[loup_3 \dots loup_5] = [lo_3 \dots lo_5]$$

The list '$loup$' is the combination of lower- and upper-bit values. The first three bits in list '$loup$' is first three bits of the lower and upper lists. Follow the same steps to generate the list 'leri' for the left and right pixels as shown in the Equation (5).

$$[leri_0 \dots leri_2] = [le_0 \dots le_2] \oplus [ri_0 \dots ri_2] \quad (5)$$

$$[leri_3 \dots leri_5] = [le_3 \dots le_5]$$

Perform OR operation between the lists '$uplo$', '$leri$' to generate the six-bit values of first channel (c1) and between lists 'rile', '$uplo$' to generate the second channel (c2) values as given in Equations (6) and (7). The centre six-bit values are directly provided to the third channel (ce).

$$[c1]_0^5 = [uplo]_0^5 || [leri]_0^5 \quad (6)$$

$$[c2]_0^5 = [rile]_0^5 || [loup]_0^5 \quad (7)$$

Generate the decimal value of the channels using Equations (8) to (10)

$$Vc1 = \sum_{i=0}^{5} c1\,(i) * 2^i \quad (8)$$

$$Vc2 = \sum_{i=0}^{5} c2\,(i) * 2^i \quad (9)$$

$$Vce = \sum_{i=0}^{5} ce\,(i) * 2^i \quad (10)$$

Generate the mean value of the pattern using Equation (11)

$$Mean = (V_{c1} + V_{c2} + V_{ce})/3 \quad (11)$$

Normalize the obtained pattern by using mean and standard deviation value. The normalized pattern is given by

$$Pattern' = \frac{Pattern - Mean}{Standard\ Deviation} \quad (12)$$

Where standard deviation is the difference between mean of the squared pattern and square of the mean value. Repeat the procedure for all pixels in the input lung nodule slices

3.3.2 Directional Hexagonal Inter-Intra Mixed Pattern

The DHIIMP pattern follows the same procedure as DHIMP, except for selecting adjacent neighboring pixels. The center pixel value is chosen from a particular cell in the CT image. The remaining left, right, upper, and lower values are chosen from the PET and CT images, forming a fused pattern.

x-4,y-4	x-4,y-3	x-4,y-2	x-4,y-1	P(x-4,y)	x-4,y+1	x-4,y+2	x-4,y+3	x-4,y+4
x-3,y-4	x-3,y-3	x-3,y-2	P(x-3,y-1)	x-3,y	P(x-3,y+1)	x-3,y+2	x-3,y+3	x-3,y+4
x-2,y-4	x-2,y-3	x-2,y-2	C(x-2,y-1)	C(x-2,y)	C(x-2,y+1)	x-2,y+2	x-2,y+3	x-2,y+4
x-1,y-4	C(x-1,y-3)	P(x-1,y-2)	C(x-1,y-1)	C(x-1,y)	C(x-1,y+1)	P(x-1,y+2)	C(x-1,y+3)	x-1,y+4
C(x,y-4)	x,y-3	x,y-2	P(x,y-1)	C(x,y)	P(x,y+1)	x,y+2	x,y+3	C(x,y+4)
x+1,y-4	C(x+1,y-3)	P(x+1,y-2)	C(x+1,y-1)	C(x+1,y)	C(x+1,y+1)	P(x+1,y+2)	C(x+1,y+3)	x+1,y+4
x+2,y-4	x+2,y-3	x+2,y-2	C(x+2,y-1)	C(x+2,y)	C(x+2,y+1)	x+2,y+2	x+2,y+3	x+2,y+4
x+3,y-4	x+3,y-3	x+3,y-2	P(x+3,y-1)	x+3,y	P(x+3,y+1)	x+3,y+2	x+3,y+3	x+3,y+4
x+4,y-4	x+4,y-3	x+4,y-2	x+4,y-1	P(x+4,y)	x+4,y+1	x+4,y+2	x+4,y+3	x+4,y+4

Figure 5. Pixel selection in Directional Hexagonal Inter-Intra Mixed Pattern

Figure. 5 clearly shows the selection of all five sets of hexagonal bits by fusing the pixels in both PET and CT images. From Figure .4, C (x, y) is the center pixels selected from the CT scan images and P (x, y) denote the pixels selected from the PET scan images. The mixed pattern obtained covers the edge pixels, which may have the important information about the malignancy which is often missed by other pattern generators.

3.4 Mlsia Network Model

This section clearly explains the multi-level self and inter-attention (MLSIA) network model, which effectively classifies lung cancer into four categories.

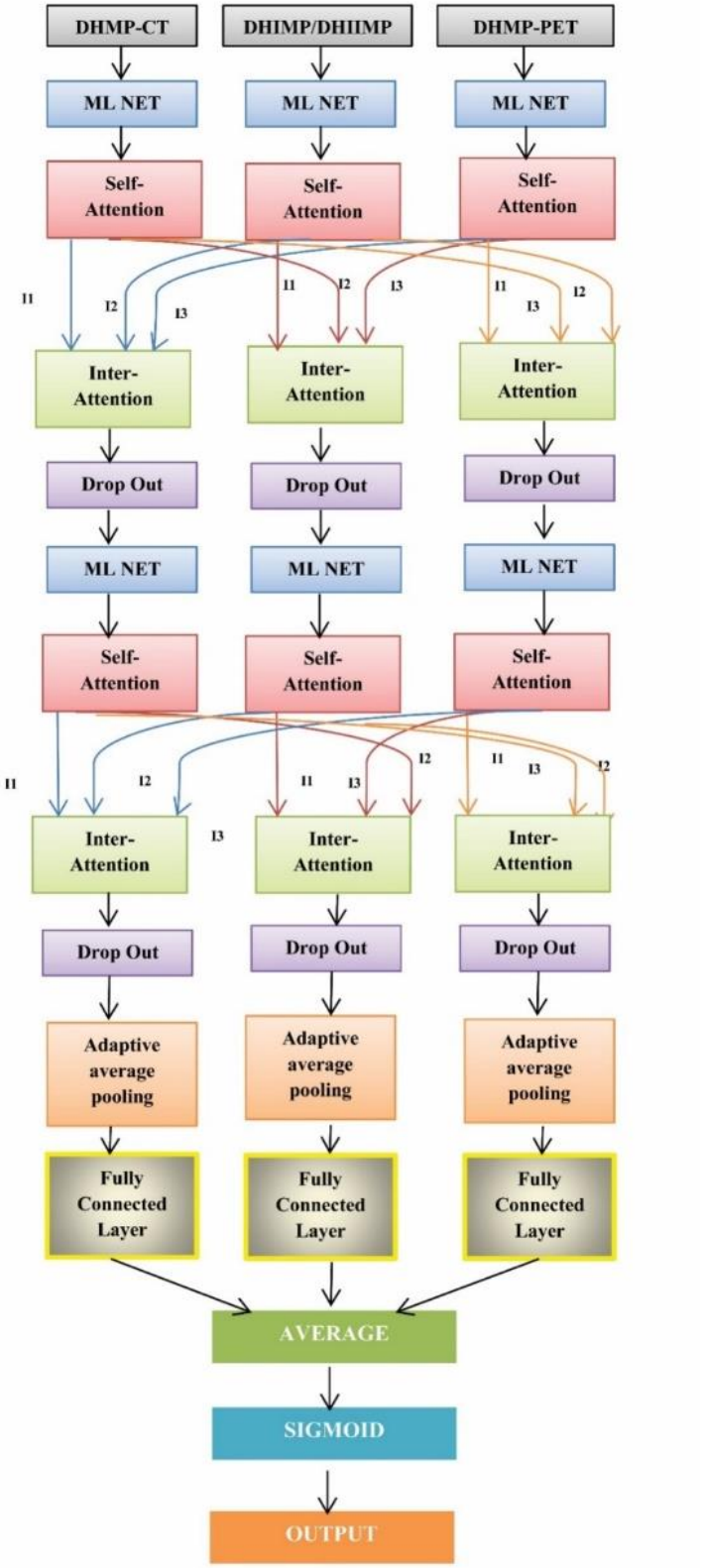

Figure 6. Multi-Level Self Attention-Inter Attention network model

The network model has three parallelly connected network architectures; each network gets a different texture pattern as input. A clear representation of MLSIA network is given in Figure 6. The network model consists of three parallelly connected architectures, each having two levels of ML Net and SA Net followed by the Inter Attention levels.

4 RESULT AND CONCLUSION

This section briefly discusses about results obtained by the MLSIA network model with the DHMP, DHIMP, and DHIIMP pattern generation algorithms. We also compare the results of both the MLSA and MLSIA network model with the PET and CT scan images.

4.1 Performance analysis

The performance of the MLSA and MLSIA classifiers are analyzed based on the performance metrics like accuracy, precision, recall, and Fl score. Table .1 shows the comparison between the MLSA network model with DHMP, and the proposed model MLSIA with DHIMP and DHIIMP patterns. Here, the MLSIA network model with DHIIMP texture pattern has achieved good results on Lung-PET-CT-DX TCIA database.

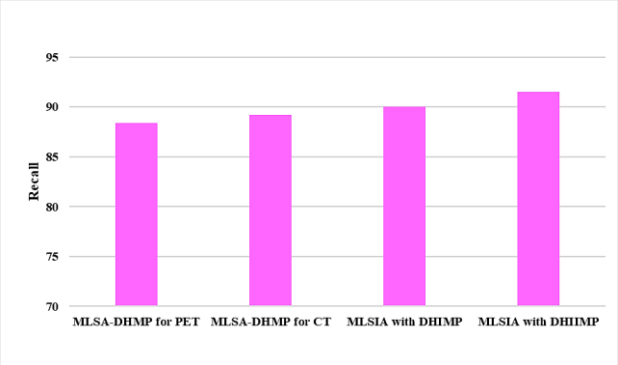

Figure 7. Graphical representation of accuracy measure for proposed classification models

Figure.7 depicts the recall measure comparison of proposed classification models by using PET and CT images. From this comparison, the recall achieved by MLSIA-LC is 88.4% for PET images and 89.2% for CT images. Moreover, the MLSIA-LC models attain the recall range of 90% and 91.5% respectively. MLSIA-LC models performs better than the MLSIA-LC model in terms recall measure. The MLSIA-LC improves the overall precision of 1.6% better than MLSIA-LC model.

4.2 Comparative analysis

The proposed MLSIA-LC method's accuracy and efficiency were demonstrated by comparing it to other methods that are existing in use. Accuracy, precision, F1 score, and recall measures are employed to assess the proposed approach's efficacy. The accuracy rate indicates that the proposed approach is more accurate than existing approaches.

Table 1. Comparison of the performance between MLSA and MLSIA network models

Methodology	Accuracy	Precision	Recall	F1score
MLSIA-LC for PET images	90.0	85.2	88.4	86.8
MLSIA-LC for CT images	90.5	85.9	89.2	87.5
MLSIA with DHIMP	91.0	87.1	90.0	88.5
MLSIA with DHIIMP	92.1	88.5	91.5	90.0

The accuracy of the MLSIA with DHIIMP pattern is 92% which is 2% more than the MLSA with DHMP pattern and 1% high than the MLSIA with the DHIMP pattern. And also, MLSIA with DHIIMP has achieved a F1 Score of 90% which is 2.5% more than that of MLSIA with DHIMP. This shows that, inter and intra mixing of patterns obtained by combining PET and CT in all the directions has enhanced the performance of MLSIA network model.

5. CONCLUSION

In this research, a novel MLSIA-LC model is proposed for the classification of Lung cancer. Initially, the LC-input images CT and PET are fed in to Attention U-Net to segment lung nodules. Advanced texture patterns, namely Directional Hexagonal Inter Mixed Pattern (DHIMP) and Directional Hexagonal Inter-Intra Mixed Pattern (DHIIMP), are extracted from segmented regions to capture unique spatial features from both CT and PET images. These patterns are fed into a parallel network architecture comprising three pathways, each with two levels of Multi-Level Self-Attention (MLSA) networks and Inter-Attention layers, followed by dropout mechanisms to enhance feature. The experimental results of MLSIA-LC network achieves higher classification performance compared to existing methods, particularly with the DHIIMP texture pattern. The proposed model achieved an accuracy of 92.1% and an F1 score of 90%, outperform effectively leveraging inter- and intra-pattern information. Future work will focus on integrating multi-modal data, such as genomic profiles and clinical records, with imaging techniques to enhance classification accuracy and enable personalized lung cancer treatment. Additionally, real-time deployment of the model in clinical settings will be explored

CONFLICTS OF INTEREST

No financial or interpersonal conflicts have been reported by the authors that would have affected the study's findings.

FUNDING STATEMENT

Neither public, private, nor nonprofit organizations provided funding for this research.

ACKNOWLEDGMENTS

The author would like to express his heartfelt gratitude to the supervisor for his guidance and unwavering support during this research for his guidance and support.

REFERENCES

[1] V.T. Ponnada, and S.N. Srinivasu, “Efficient CNN for Lung Cancer Detection”, *International Journal of Recent Technology and Engineering*, vol. 8, pp. 3499-3505, 2020. [CrossRef] [Google Scholar] [Publisher Link]

[2] K. Punithavathy, M.M. Ramya, and S. Poobal, “Analysis of statistical texture features for automatic lung cancer detection in PET/CT images”, *In 2015 International Conference on Robotics, Automation, Control and Embedded Systems*

(RACE), pp. 1-5, 2015. [CrossRef] [Google Scholar] [Publisher Link]

[3] R. Qin, Z. Wang, L. Jiang, K. Qiao, J. Hai, J. Chen, J. Xu, D. Shi, and B. Yan, "Fine-grained lung cancer classification from PET and CT images based on multidimensional attention mechanism", *Complexity*, 2020. [CrossRef] [Google Scholar] [Publisher Link]

[4] D. Riquelme, and M.A. Akhloufi, "Deep learning for lung cancer nodules detection and classification in CT scans", Ai, vol. 1, no. 1, pp. 28-67, 2020. [CrossRef] [Google Scholar] [Publisher Link]

[5] M. Roemer, "Cancer-Related Hospitalizations for Adults", 2017: Statistical Brief# 270, 2021. [CrossRef] [Google Scholar] [Publisher Link]

[6] S.D. Roy, S. Das, D. Kar, F. Schwenker, and R. Sarkar. "Computer aided breast cancer detection using ensembling of texture and statistical image features", *Sensors*, vol. 21, no. 11, pp. 3628, 2021[CrossRef] [Google Scholar] [Publisher Link]

[7] M.M. Saab, B. Noonan, C. Kilty, S. FitzGerald, A. Collins, A. Lyng, U. Kennedy, M. O'Brien, and J. Hegarty, "Awareness and help-seeking for early signs and symptoms of lung cancer: A qualitative study with high-risk individuals", *European Journal of Oncology Nursing*, vol. 50, pp. 101880, 2021. [CrossRef] [Google Scholar] [Publisher Link]

[8] P. Sardarabadi, A.A. Kojabad, D. Jafari, and C.H. Liu, "Liquid biopsy-based biosensors for MRD detection and treatment monitoring in Non-Small Cell Lung Cancer (NSCLC)". *Biosensors,* vol. 11, no. 10, pp. 394, 2021. [CrossRef] [Google Scholar] [Publisher Link]

[9] M. Šarić, M. Russo, M. Stella, and M. Sikora, "CNN-based method for lung cancer detection in whole slide histopathology images", *In 2019 4th International Conference on Smart and Sustainable Technologies (SpliTech),* pp. 1-4, 2019. [CrossRef] [Google Scholar] [Publisher Link]

[10] M. Schwyzer, D.A. Ferraro, U.J. Muehlematter, A. Curioni-Fontecedro, M.W. Huellner, G.K. Von Schulthess, P.A. Kaufmann, I.A. Burger, and M. Messerli, "Automated detection of lung cancer at ultralow dose PET/CT by deep neural networks–initial results", *Lung Cancer*, vol. 126, pp. 170-173, 2018. [CrossRef] [Google Scholar] [Publisher Link]

[11] R.D. Seeja, and A. Suresh, "Melanoma classification employing inter neighbor statistical color and mean order pattern texture feature", *Multimedia Tools and Applications,* vol. 80, no. 13, pp. 20045-20064, 2021. [CrossRef] [Google Scholar] [Publisher Link]

[12] K. Shak, M. Al-Shabi, A. Liew, B.L. Lan, W.Y. Chan, K.H. Ng, and M. Tan, "A new semi-supervised self-training method for lung cancer prediction", 2020. [CrossRef] [Google Scholar] [Publisher Link]

[13] A. Srivastava, D. Jha, S. Chanda, U. Pal, H.D. Johansen, D. Johansen, M.A. Riegler, S. Ali, and P. Halvorsen. "Msrf-net: A multi-scale residual fusion network for biomedical image segmentation", *IEEE Journal of Biomedical and Health Informatics*, vol. 26, no. 5, pp. 2252-2263, 2021. [CrossRef] [Google Scholar] [Publisher Link]

[14] R. Wulandari, R. Sigit, and S. Wardhana, "Automatic lung cancer detection using color histogram calculation", *In 2017 International Electronics Symposium on Knowledge Creation and Intelligent Computing (IES-KCIC),* pp. 120-126, 2017[CrossRef] [Google Scholar] [Publisher Link]

[15] M. Nishio, C. Nagashima, S. Hirabayashi, A. Ohnishi, K. Sasaki, T. Sagawa, M. Hamada, and T. Yamashita. "Convolutional auto-encoder for image denoising of ultra-low-dose CT", Heliyon, vol. 3, no. 8, pp. 00393, 2017. [CrossRef] [Google Scholar] [Publisher Link]

[16] S. Perumal, and T. Velmurugan, "Preprocessing by contrast enhancement techniques for medical images", *International Journal of Pure and Applied Mathematics*, vol. 118, no. 18, pp. 3681-3688, 2018. [CrossRef] [Google Scholar] [Publisher Link]

[17] P.M. Shakeel, M.A. Burhanuddin, and M.I. Desa. "Automatic lung cancer detection from CT image using improved deep neural network and ensemble classifier", *Neural Computing and Applications*, pp. 1-14, 2020. [CrossRef] [Google Scholar] [Publisher Link]

[18] E. Tasci, C. Uluturk, and A. Ugur, "A voting-based ensemble deep learning method focusing on image augmentation and preprocessing variations for tuberculosis detection", *Neural Computing and Applications,* vol. 33, no. 22, pp. 15541-15555, 2021. [CrossRef] [Google Scholar] [Publisher Link]

[19] W.J. Sori, J. Feng, A.W. Godana, S. Liu, and D.J. Gelmecha. "DFD-Net: lung cancer detection from denoised CT scan image using deep learning", *Frontiers of Computer Science*, vol. 15, no. 2, pp. 1-13, 2021[CrossRef] [Google Scholar] [Publisher Link]

[20] M.B.A. Miah, and M.A. Yousuf, "Detection of lung cancer from CT image using image processing and neural network", *In 2015 International conference on electrical engineering and information communication technology (ICEEICT),* pp. 1-6, 2015. [CrossRef] [Google Scholar] [Publisher Link]

AUTHORS

P. William is working as Director (Research) at Sanjivani University, Kopargaon. He is the Post Doctoral Fellow from Amity University Dubai, UAE and Adjunct faculty of Victorian Institute of Technology, Australia. He is recognized in World Top 2% Scientist list by Stanford University and Elsevier. He is a member of IEEE, QCFI, ISTE and various other professional bodies. His research includes innovation and development of cutting-edge solutions in the fields of natural language processing, artificial intelligence, deep learning, machine learning, soft computing, cybersecurity, and cloud computing. He has published 225+ papers in Scopus indexed journals and Conferences. He has 30+ patents published with grants in his credit. He has authored and edited 20+ books with renowned publishers of global recognition. He has been associated with numerous Multi-National Companies and various Educational Groups for his expertise in research, corporate training and consulting where he has contributed to the advancement of knowledge and practice in his domain. A focused professional with experience of consulting in Research, Innovation and Development. He served as a Chairperson and Auditor in multiple committees of national recognition. Delivered Keynotespeeches and chaired many sessions in International Conferences.

Abdulatif Alabdulatif is an associate professor at the School of Computer Science & IT, Qassim University, Saudi Arabia. He completed his Ph.D. degree in Computer Science from RMIT University, Australia in 2018. He received his B.Sc. degree in Computer Science from Qassim University, Saudi Arabia in 2008 and his M.Sc. degree in Computer Science from RMIT University, Australia in 2013. He has published more than 70 academic papers in prominent journals. His research interests include applied cryptography, cloud computing, and E-health

Arrived: 19.01.2024
Accepted: 22.02.2024